A SHEAR-LAG ANALYSIS OF STRESS TRANSFER THROUGH A COHESIVE FIBRE-MATRIX INTERFACE

Zuorong Chen[1] and Wenyi Yan[2]

[1] CSIRO Energy Flagship, Private Bag 10, Clayton South, Victoria 3168, Australia.
Email address: zuorong.chen@csiro.au. Website: www.csiro.au

[2] Department of Mechanical and Aerospace Engineering, Monash University, Wellington Road, Clayton, Victoria 3800, Australia.
Email address: wenyi.yan@monash.edu. Website: www.monash.edu

Keywords: Shear-lag, Cohesive interface, Stress transfer, Interfacial debonding

ABSTRACT

A shear-lag model with a cohesive fibre-matrix interface is presented for the analysis of stress transfer between the fibre and the matrix in unidirectional fibre-reinforced composites. The fibre–matrix interface is described by an irreversible bilinear cohesive traction-separation law. The interface is initially perfectly bonded and linear elastic. Beyond the elastic deformation regime during fibre pull-out, interfacial damage initiates and evolves progressively, exhibiting a reduction in the shear strength and a degradation of the shear stiffness. The governing equations for the interfacial shear stress and the axial stress in the fibre are derived. Analytical solutions of stress distribution and evolution are obtained using a shear strength-based debonding criterion. Depending on the parameters of the fibre-matrix-cohesive interface system, the stresses in the cohesive interface damage process zone may obey two different types of governing equations.

1 INTRODUCTION

Owing to their extraordinary mechanical properties and interesting thermal, electrical, and optical properties, one-dimensional carbon nanotubes and two-dimensional graphene sheets have shown promise for a wide range of applications as mechanical reinforcements in high-performance structural composite materials or as functional components in flexible electronics and multifunctional devices [1-4]. The interfacial bonding between the carbon nanotube or graphene sheet and the matrix determines how effectively their outstanding physical properties can be utilised. So the load transfer and deformation mechanisms in these composites and functional devices have attracted considerable attention and investigations [5-8]. The classical shear-lag model has been adopted whether in experimental characterisation of the interfacial mechanical properties [7, 8] or in numerical and theoretical modelling of the stress distribution and evolution and the interfacial debonding process with introducing a cohesive damage process zone model [9-18]. In this paper, we present a shear-lag model with a cohesive fibre-matrix interface for the analysis of the stress transfer and deformation process. The interfacial debonding is modelled by an irreversible bilinear cohesive traction-separation law. Analytical relationships between the distribution and evolution of stresses and deformation and the interfacial cohesive properties are established.

2 A SHEAR-LAG MODEL WITH AN IRREVERSIBLE FIBRE-MATRIX INTERFACE

As shown in Figure 1, a composite cylinder model is adopted for the analysis of the load transfer between the fibre and the matrix through an irreversible cohesive interface. A single fibre with a radius a is embedded and initially perfectly bonded with a length L in a coaxial cylinder with an outer radius of b. The embedded end face $(z = 0)$ of the fibre can be perfectly bonded with or completely free from the matrix, and an axial tensile stress σ_p is applied to the end face $(z = l)$ of the fibre. It is assumed that both the fibre and matrix are elastic, and the load is transferred purely by interfacial shear between them. The outer surface $(r = b)$ of the matrix cylinder is free from stress.

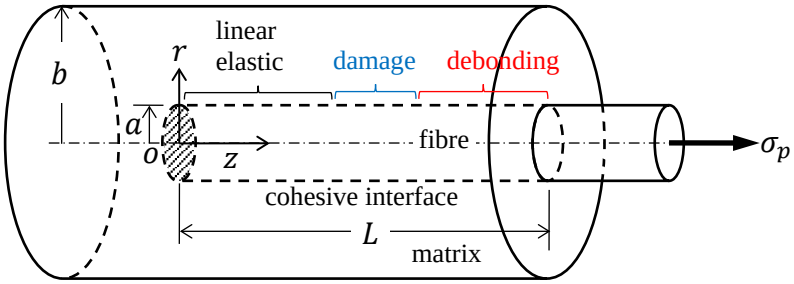

Figure 1: A composite fibre-matrix cylinder model with a cohesive interface.

The interface $(r = a)$ between the fibre and matrix is modelled as a cohesive interface in pure shear mode which is described by an irreversible bilinear cohesive traction-separation law. As shown in Figure 2, the cohesive law is characterised by an initial linear elastic regime of an initial shear stiffness K_0 followed by a linear softening regime which exhibits both a reduction in the shear strength and a degradation of the shear stiffness. Interfacial damage initiates once the interfacial shear stress reaches the cohesive shear strength τ_0 and the shear separation reaches the critical value δ_0. Beyond this point, as the shear separation increases further, the shear stress decreases due to material degradation until the complete failure (interfacial debonding) begins where the separation reaches the critical value δ_1 and the traction of cohesive strength acting across the cohesive interface is reduced to zero. The interfacial damage is described by the scalar damage variable D $(0 \le D \le 1)$which is a function of the maximum shear separation δ_m attained during the loading history. The limits of the damage variable correspond to an intact $(D = 0)$ and a fully debonded $(D = 1)$ cohesive interface, respectively. Within the cohesive damage process zone, any unloading and re-loading occur elastically by following a curve (different from the loading envelop) with a degraded shear stiffness $(1 - D)K_0$.

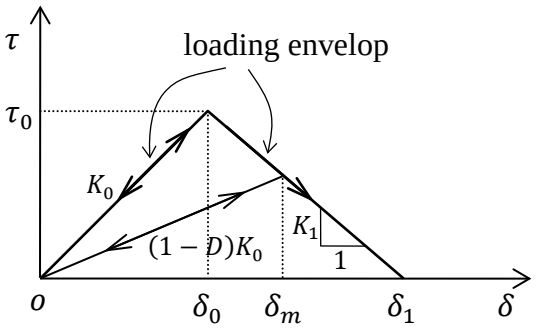

$$K_0 = \frac{\tau_0}{\delta_0}$$

$$K_1 = \frac{\tau_0}{\delta_1 - \delta_0} = \frac{\delta_0}{\delta_1 - \delta_0} K_0$$

$$D = \frac{\delta_1(\delta_m - \delta_0)}{\delta_m(\delta_1 - \delta_0)}$$

Figure 2: An irreversible bilinear cohesive traction separation law.

The irreversible bilinear cohesive traction-separation constitutive law is given by

$$\tau = \begin{cases} K_0\delta & \text{for} \quad 0 \le \delta_m \le \delta_0 \\ (1-D)K_0\delta & \text{for} \quad \delta_0 \le \delta_m \le \delta_1 \\ 0 & \text{for} \quad \delta_m \ge \delta_1 \end{cases} \tag{1}$$

Irreversibility manifests itself upon unloading and reloading after damage initiation. Within the cohesive damage process zone $(\delta_0 \le \delta_m \le \delta_1)$, loading is characterised by the conditions $\delta = \delta_m$ and $\dot{\delta} \ge 0$, and the cohesive interface undergoes unloading for $\delta < \delta_m$ and $\dot{\delta} < 0$ and reloading for $\delta < \delta_m$ and $\dot{\delta} \ge 0$. Then we have

$$\tau = \left[1 - \frac{\delta_1(\delta_m - \delta_0)}{\delta_m(\delta_1 - \delta_0)}\right] K_0\delta = K_1(\delta_1 - \delta) \qquad \text{for } \delta = \delta_m \text{ and } \dot{\delta} \ge 0 \text{ (loading)} \tag{2}$$

and

$$\tau = \left[1 - \frac{\delta_1(\delta_m - \delta_0)}{\delta_m(\delta_1 - \delta_0)}\right] K_0\delta = K_1\delta\left(\frac{\delta_1}{\delta_m} - 1\right) \qquad \text{for } \delta < \delta_m \text{ (unloading or re-loading)} \quad (3)$$

where $\dot{\delta}$ is the rate or incremental of the shear separation.

The transversely isotropic linear thermoelastic constitutive relations for the fibre and matrix are:

$$\varepsilon_{zz} = \frac{\sigma_{zz}}{E_A} - \frac{\nu_A}{E_A}(\sigma_{rr} + \sigma_{\theta\theta}) + \alpha_A T, \qquad \gamma_{rz} = \frac{\tau_{rz}}{G_A}, \quad (4)$$

where E_A, G_A, ν_A, and α_A are the tensile modulus, shear modulus, Poisson's ratio, and thermal expansion coefficient in the longitudinal direction, respectively, and T is the temperature difference from the stress-free temperature T_0.

The following axial equilibrium equation must be satisfied in both the fibre and the matrix

$$\frac{\partial\sigma_{zz}}{\partial z} + \frac{1}{r}\frac{\partial(r\tau_{rz})}{\partial r} = 0. \quad (5)$$

According to the fundamental shear-lag assumption, the axial tensile and shear strains are given in terms of the axial displacement $w(r,z)$, respectively, by

$$\varepsilon_{zz} = \frac{\partial w}{\partial z}, \qquad \text{and} \qquad \gamma_{rz} = \frac{\partial w}{\partial r}. \quad (6)$$

The shear stress distribution in the fibre and matrix are assumed to be of the form [19, 20]

$$\tau_{rz}^f(r,z) = \tau_a(z)I(r) \qquad \text{and} \qquad \tau_{rz}^m(r,z) = \tau_a(z)O(r) \quad (7)$$

where the superscripts f and m denote the fibre and matrix, respectively. $\tau_a(z)$ is the axial shear stress at the interface. The functions $I(r)$ and $O(r)$ define the assumed radial dependence of the shear stress in the fiber and the matrix, respectively, which satisfy the continuity and boundary conditions

$$I(0) = 0,\ I(a) = 1,\ O(a) = 1, \text{ and } O(b) = 0 \quad (8)$$

The axial displacement of the fibre and matrix at $r = a$ and the shear separation (δ) of the cohesive interface satisfy the following deformation relation

$$w^f(a,z) - w^m(a,z) = \delta(z) \quad (9)$$

The differential equations that determine the average axial tensile stress in the fibre, $\sigma_f(z)$, can be obtained as

$$\frac{d\sigma_f(z)}{dz} = -\frac{2\tau_a(z)}{a} \quad (10)$$

$$\frac{d^2\sigma_f(z)}{dz^2} = \frac{\left[\frac{1}{\left(\frac{b^2}{a^2}-1\right)} + \frac{E_A^m}{E_A^f}\right]}{a^2E_A^m\left\{\frac{\left[\frac{r}{a}I(r)\right]}{4G_A^f} + \frac{\left[\left(\frac{b^2}{r^2}-1\right)\frac{r}{a}O(r)\right]}{4G_A^m}\right\}}\left\{\sigma_f(z) - \frac{\sigma_p}{\left[1+\left(\frac{b^2}{a^2}-1\right)\frac{E_A^m}{E_A^f}\right]} - \frac{E_A^m\left(\frac{b^2}{a^2}-1\right)}{\left[1+\left(\frac{b^2}{a^2}-1\right)\frac{E_A^m}{E_A^f}\right]}\left[\frac{d\delta(z)}{dz} + \left(\alpha_A^m - \alpha_A^f\right)T\right]\right\} \quad (11)$$

The detailed derivation of Eqs. (10) and (11) can be found in our previous work [16]. The irreversible traction-separation cohesive law Eqs. (1)-(3) and the differential equations (10) and (11) form the governing equations for the irreversible cohesive-shear-lag model, from which the distribution and evolution of the stress can be solved when subjected to given boundary conditions.

3 DISTRIBUTION AND EVOLUTIONOF INTERFACIAL STRESS

The distributions and evolutions of the axial tensile stress in the fibre, the interfacial shear stress and separation for the cohesive interface in different deformation regimes are given below. The coordinates as shown in Figure 3 have been used for different deformation zones.

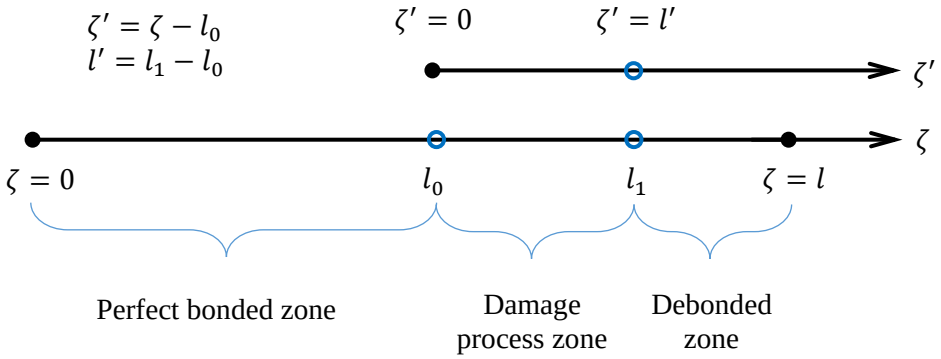

Figure 3: Different deformation zones and coordinates.

In this paper, for the sake of simplicity, we consider the case that damage and debonding always initiate at the loaded end (the right end) of the fibre and develop leftwards. More complex scenarios that the damage and debonding may initiate and evolve from either end in different orders have been discussed in our previous work [16].

3.1 Initial linear elastic regime

For the cohesive interface in the initial linear elastic deformation regime, it can be obtained from Eqs. (1) and (10) that

$$\frac{d\delta(z)}{dz} = \frac{1}{K_0}\frac{d\tau(z)}{dz} = -\frac{1}{K_0}\frac{d\tau_a(z)}{dz} = \frac{a}{2K_0}\frac{d^2\sigma_f(z)}{dz^2} \tag{12}$$

where $\tau(z)$ is the shear traction in the cohesive interface, and $\tau(z) = -\tau_a(z)$.

Substituting Eq. (12) into Eq. (11) results in the governing equation expressed in terms of the average axial stress in the fibre as

$$\frac{d^2\sigma_f(z)}{dz^2} = \frac{2\left(\frac{a^2}{b^2-a^2}+\frac{E_A^m}{E_A^f}\right)}{a^2\left[\frac{E_A^m}{2G_A^f}\overline{\left[\frac{r}{a}I(r)\right]}+\frac{E_A^m}{2G_A^m}\overline{\left[\left(\frac{b^2}{r^2}-1\right)\frac{r}{a}O(r)\right]}+\frac{E_A^m}{aK_0}\right]}\left\{\sigma_f(z) - \frac{1}{\left[1+\frac{E_A^m}{E_A^f}\left(\frac{b^2}{a^2}-1\right)\right]}\sigma_p - \sigma_T\right\} \tag{13}$$

where $\sigma_T = \frac{E_A^m\left(\alpha_A^m-\alpha_A^f\right)T}{\frac{a^2}{b^2-a^2}+\frac{E_A^m}{E_A^f}}$.

Introduce the following scaling parameters: $\zeta = z/a$, $l = L/a$, $\gamma = 1\Big/\left[1+\frac{E_A^m}{E_A^f}\left(\frac{b^2}{a^2}-1\right)\right]$, and define the cohesive-shear-lag parameter

$$\alpha = \left\{\frac{2\left[\frac{1}{(b^2/a^2-1)}+\frac{E_A^m}{E_A^f}\right]}{\frac{E_A^m}{2G_A^f}\overline{\left[\frac{r}{a}I(r)\right]}+\frac{E_A^m}{2G_A^m}\overline{\left[\left(\frac{b^2}{r^2}-1\right)\frac{r}{a}O(r)\right]}+\frac{E_A^m}{aK_0}}\right\}^{1/2} \tag{14}$$

Then, the governing equation Eq. (13) can be expressed as:

$$\frac{d^2\sigma_f(\zeta)}{d\zeta^2} = \alpha^2\left[\sigma_f(\zeta) - \gamma\sigma_p - \sigma_T\right] \tag{15}$$

and the interfacial shear stress is

$$\tau_a(\zeta) = -\frac{1}{2}\frac{d\sigma_f(\zeta)}{d\zeta} \tag{16}$$

Define the following boundary conditions:

$$\sigma_f(\zeta = 0) = \epsilon\sigma_p, \quad \sigma_f(\zeta = l) = \sigma_p \tag{17}$$

where the dimensionless factor ϵ defines the relation between the applied load, σ_p, and the average fibre axial stress at the embedded end face ($\zeta = 0$).

Solution of Eq. (15) subjected to the boundary conditions Eq. (17) yields, for the case of $\sigma_T = 0$,

$$\sigma_f = \sigma_p\varphi_0(\zeta, l, \alpha) \qquad \tau_a = -\frac{\sigma_p}{2}\omega_0(\zeta, l, \alpha) \qquad \delta = \frac{\sigma_p}{2K_0}\omega_0(\zeta, l, \alpha) \tag{18}$$

where

$$\varphi_0(\zeta, l, \alpha) = \frac{\mathrm{Sinh}(\alpha\zeta)}{\mathrm{Sinh}(\alpha l)} - \epsilon\frac{\mathrm{Sinh}[\alpha(\zeta - l)]}{\mathrm{Sinh}(\alpha l)} + \gamma\left[1 - \frac{\mathrm{Sinh}(\alpha\zeta) - \mathrm{Sinh}[\alpha(\zeta - l)]}{\mathrm{Sinh}(\alpha l)}\right]$$
$$\omega_0(\zeta, l, \alpha) = \varphi_0'(\zeta, l, \alpha) = \alpha\left\{\frac{\mathrm{Cosh}(\alpha\zeta)}{\mathrm{Sinh}(\alpha l)} - \epsilon\frac{\mathrm{Cosh}[\alpha(\zeta - l)]}{\mathrm{Sinh}(\alpha l)} - \gamma\frac{\mathrm{Cosh}(\alpha\zeta) - \mathrm{Cosh}[\alpha(\zeta - l)]}{\mathrm{Sinh}(\alpha l)}\right\} \tag{19}$$

The critical load for the damage initiation at $\zeta = l$ is given by

$$\delta(\zeta = l) = \delta_0 \ \rightarrow \sigma_p^0(l) = \frac{2K_0\delta_0}{\omega_0(l,l,\alpha)} \tag{20}$$

As the damage process zone develops, the length of the linear elastic deformation zone decreases, and the solution of the perfectly bonded zone can still be expressed by Eqs. (18) and (19) with the length of the elastic deformation zone l being replaced by l_0.

3.2 Damage process zone – monotonic loading

For the irreversible cohesive law as shown in Figure 2, the interface in the cohesive damage process zone behaves differently under loading, unloading and reloading conditions. Under the condition of monotonic loading and no local unloading, it can be obtained from Eq. (2)

$$\frac{d\delta}{dz} = -\frac{1}{K_1}\frac{d\tau}{dz} = \frac{1}{K_1}\frac{d\tau_a(z)}{dz} = -\frac{a}{2K_1}\frac{d^2\sigma_f(z)}{dz^2} \tag{21}$$

Substituting Eq. (21) into Eq. (11) results in the differential equation expressed in terms of the average axial stress in the fibre as

$$\frac{d^2\sigma_f(z)}{dz^2} = \frac{2\left(\frac{a^2}{b^2-a^2} + \frac{E_A^m}{E_A^f}\right)}{a^2\left[\frac{E_A^m}{2G_A^f}\overline{\left[\frac{r}{a}I(r)\right]} + \frac{E_A^m}{2G_A^m}\overline{\left[\left(\frac{b^2}{r^2} - 1\right)\frac{r}{a}O(r)\right]} - \frac{E_A^m}{aK_1}\right]}\left\{\sigma_f(z) - \frac{1}{\left[1 + \frac{E_A^m}{E_A^f}\left(\frac{b^2}{a^2} - 1\right)\right]}\sigma_p - \sigma_T\right\} \tag{22}$$

Define the dimensionless parameter

$$\beta = \left\{\frac{2\left[\frac{1}{(b^2/a^2-1)} + \frac{E_A^m}{E_A^f}\right]}{\left|\frac{E_A^m}{2G_A^f}\overline{\left[\frac{r}{a}I(r)\right]} + \frac{E_A^m}{2G_A^m}\overline{\left[\left(\frac{b^2}{r^2} - 1\right)\frac{r}{a}O(r)\right]} - \frac{E_A^m}{aK_1}\right|}\right\}^{1/2} \quad \text{for } \frac{E_A^m}{2G_A^f}\overline{\left[\frac{r}{a}I(r)\right]} + \frac{E_A^m}{2G_A^m}\overline{\left[\left(\frac{b^2}{r^2} - 1\right)\frac{r}{a}O(r)\right]} - \frac{E_A^m}{aK_1} \neq 0 \tag{23}$$

Then, we have the dimensionless forms of Eq. (22) for the two different cases, respectively, as

$$\frac{d^2\sigma_f(\zeta)}{d\zeta^2} = -\beta^2\left[\sigma_f(\zeta) - \gamma\sigma_p - \sigma_T\right] \quad \text{for} \quad \frac{E_A^m}{2G_A^f}\overline{\left[\frac{r}{a}I(r)\right]} + \frac{E_A^m}{2G_A^m}\overline{\left[\left(\frac{b^2}{r^2} - 1\right)\frac{r}{a}O(r)\right]} - \frac{E_A^m}{aK_1} < 0 \tag{24}$$

$$\frac{d^2\sigma_f(\zeta)}{d\zeta^2} = \beta^2\left[\sigma_f(\zeta) - \gamma\sigma_p - \sigma_T\right] \quad \text{for} \quad \frac{E_A^m}{2G_A^f}\overline{\left[\frac{r}{a}I(r)\right]} + \frac{E_A^m}{2G_A^m}\overline{\left[\left(\frac{b^2}{r^2} - 1\right)\frac{r}{a}O(r)\right]} - \frac{E_A^m}{aK_1} > 0 \tag{25}$$

Further, differentiating Eqs. (24) and (25) and using Eqs. (21), (10) and (2) results in the differential equations expressed in terms of the shear separation, respectively, as

$$\frac{d^2\delta(\zeta)}{d\zeta^2} = -\beta^2[\delta(\zeta) - \delta_1] \quad \text{for} \quad \frac{E_A^m}{2G_A^f}\overline{\left[\frac{r}{a}I(r)\right]} + \frac{E_A^m}{2G_A^m}\overline{\left[\left(\frac{b^2}{r^2} - 1\right)\frac{r}{a}O(r)\right]} - \frac{E_A^m}{aK_1} < 0 \tag{26}$$

$$\frac{d^2\delta(\zeta)}{d\zeta^2} = \beta^2[\delta(\zeta) - \delta_1] \quad \text{for} \quad \frac{E_A^m}{2G_A^f}\overline{\left[\frac{r}{a}I(r)\right]} + \frac{E_A^m}{2G_A^m}\overline{\left[\left(\frac{b^2}{r^2} - 1\right)\frac{r}{a}O(r)\right]} - \frac{E_A^m}{aK_1} > 0 \tag{27}$$

Before the appearance of the debonded zone, we have the boundary conditions for the damage process zone $(0 \le \zeta' \le l')$ as

$$\delta(\zeta' = 0) = \delta_0 \quad \delta(\zeta' = l') = \delta_p \quad \sigma_f(\zeta' = 0) = \sigma_p^0(l_0) \qquad \sigma_f(\zeta' = l') = \sigma_p \tag{28}$$

The solution of Eq. (26) subjected to the boundary conditions Eq. (28) yields, for the case of $\sigma_T = 0$

$$\sigma_f = \sigma_p^0(l_0)\varphi_1(\zeta', l', \beta) \qquad \tau_a = -\tau_0\omega_1(\zeta', l', \beta) \qquad \delta = \delta_1 - \frac{\tau_0}{K_1}\omega_1(\zeta', l', \beta) \tag{29}$$

where

$$\varphi_1(\zeta', l', \beta) = \frac{\frac{\delta_1 - \delta_p}{\delta_1 - \delta_0} - \cos(\beta l')}{\sin(\beta l')}\frac{2\tau_0}{\beta\sigma_p^0(l_0)}[1 - \cos(\beta\zeta')] + \frac{2\tau_0}{a\beta\sigma_p^0(l_0)}\sin(\beta\zeta') + 1$$

$$\omega_1(\zeta', l', \beta) = \frac{\frac{\delta_1 - \delta_p}{\delta_1 - \delta_0} - \cos(\beta l')}{\sin(\beta l')}\sin(\beta\zeta') + \cos(\beta\zeta') \tag{30}$$

The relation between the applied separation δ_p $\left(\delta_0 < \delta_p \le \delta_1\right)$and the length l' of the damage process zone is given by

$$\delta_p = \delta_1 - \frac{\gamma + (1-\gamma)\left[\cos(\beta l') - \frac{\beta\sigma_p^0(l_0)}{2\tau_0}\sin(\beta l')\right]}{1 - \gamma + \gamma\cos(\beta l')}(\delta_1 - \delta_0) \tag{31}$$

And the critical load or the critical length of the damage process zone at which the debonding initiates at $\zeta' = l'$ is determined by the condition $\delta(\zeta' = l') = \delta_1$ or equivalently $\tau(\zeta' = l') = 0$ as

$$\gamma + (1-\gamma)\left[\cos(\beta l') - \frac{\beta\sigma_p^0(l_0)}{2\tau_0}\sin(\beta l')\right] = 0 \tag{32}$$

Following the same procedure, the solution of Eq. (27) can be expressed, for the case of $\sigma_T = 0$, as

$$\sigma_f = \sigma_p^0(l_0)\varphi_1(\zeta', l', \beta) \qquad \tau_a = -\tau_0\omega_1(\zeta', l', \beta) \qquad \delta = \delta_1 - \frac{\tau_0}{K_1}\omega_1(\zeta', l', \beta) \tag{33}$$

where

$$\varphi_1(\zeta', l', \beta) = \frac{\frac{\delta_1 - \delta_p}{\delta_1 - \delta_0} - \cosh(\beta l')}{\sinh(\beta l')}\frac{2\tau_0}{\beta\sigma_p^0(l_0)}[\cosh(\beta\zeta') - 1] + \frac{2\tau_0}{a\beta\sigma_p^0(l_0)}\sinh(\beta\zeta') + 1$$

$$\omega_1(\zeta', l', \beta) = \frac{\frac{\delta_1 - \delta_p}{\delta_1 - \delta_0} - \cosh(\beta l')}{\sinh(\beta l')}\sinh(\beta\zeta') + \cosh(\beta\zeta') \tag{34}$$

The relation between the applied separation δ_p $\left(\delta_0 < \delta_p \le \delta_1\right)$and the length l' of the damage process zone is given by

$$\delta_p = \delta_1 - \frac{\gamma + (1-\gamma)\left[\cosh(\beta l') - \frac{\beta\sigma_p^0(l_0)}{2\tau_0}\sinh(\beta l')\right]}{1 - \gamma + \gamma\cosh(\beta l')}(\delta_1 - \delta_0) \tag{35}$$

And the critical load or the critical length of the damage process zone at which the debonding initiates at $\zeta' = l'$ is determined by the condition $\delta\left(\zeta^{'} = l^{'}\right) = \delta_1$ or equivalently $\tau(\zeta' = l') = 0$ as

$$\gamma + (1-\gamma)\left[\cosh(\beta l') - \frac{\beta\sigma_p^0(l_0)}{2\tau_0}\sinh(\beta l')\right] = 0 \tag{36}$$

As the debonded zone develops with further loading, the fully developed damage process zone move leftwards, and the above solutions for the damage process zone are still valid with the length of the

damage process zone l' being equal to $l_1 - l_0$.

3.3 Fully debonded zone

In the fully debonded zone, the cohesive shear stress is zero and the axial stress in the fibre is constant. So we have

$$\sigma_f(\zeta) = \sigma_p^0(l_0)\varphi_1(l_1 - l_0, l_1 - l_0, \beta) \qquad \tau_a(\zeta) = 0 \qquad (l_1 < \zeta \le l), \tag{37}$$

and the shear separation can be given by

$$\delta(\zeta) = \delta_1 + \frac{\sigma_p^0(l_0)\varphi_1(l_1 - l_0, l_1 - l_0, \beta)}{E_A^f}(\zeta - l_1) \qquad (l_1 < \zeta \le l) \tag{38}$$

The maximum pull-out force for a given embedded fibre length can be obtained from Eq. (37).

4 EXAMPLES AND DISCUSSIONS

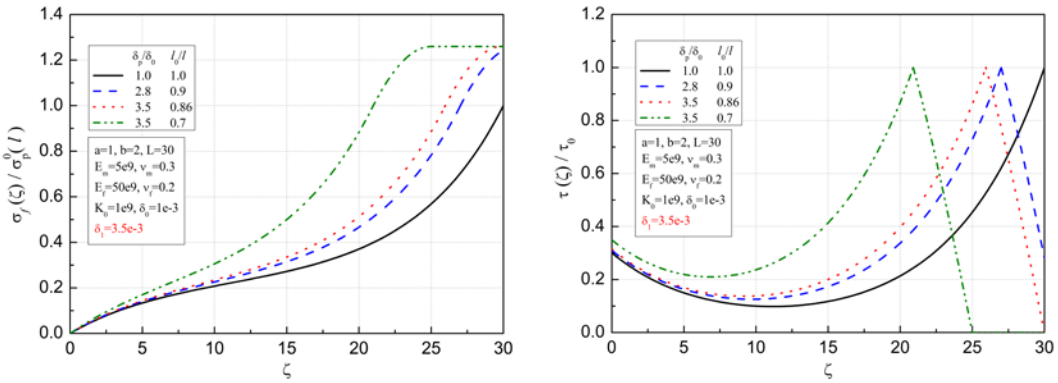

Figure 4: The distribution and evolution of the axial stress and cohesive shear stress with $\delta_1 = 0.0035$.

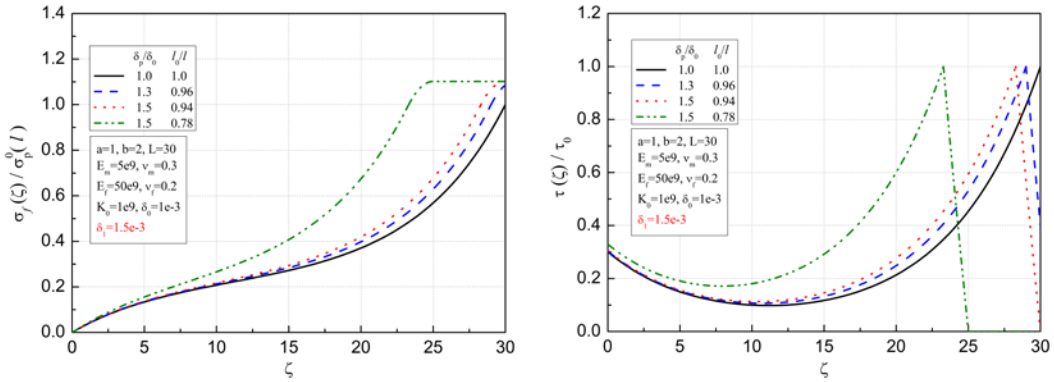

Figure 5: The distribution and evolution of the axial stress and cohesive shear stress with$\delta_1 = 0.0015$.

Figures 4 and 5 show the distribution and evolution of the axial stress in the fibre and the cohesive interfacial shear stress for two cases. The parameters used in the calculation are given in the figures. All the parameters except for δ_1 are same for the two cases. The first case (Fig 4) models a slow damage process with $K_1 = 4 \times 10^8$ which satisfies Eqs. (24) and (26), while the second case models a faster damage process with $K_1 = 2 \times 10^9$ which satisfies Eqs. (25) and (27). The length of the fully developed damage process zone in the first case is larger than that in the second case. For both case, the length of the fully developed damage process zone remains nearly unchanged as it evolves leftwards.

5 CONCLUSIONS

A cohesive shear-lag model is presented for the analysis of the stress transfer between the fibre and matrix. The interface between the fibre and matrix is modelled by an irreversible bilinear cohesive traction-separation law. Differential equations which govern the distribution and evolution of the axial stress in the fibre and the interfacial shear stress have been derived. Depending on the geometrical and mechanical properties of the cohesive-shear-lag model, the damage process zone may obey two different types of governing equations. Analytical solutions for the distribution and evolution of the stresses and separation and the lengths of different deformation zones have been obtained, which can serve as a theoretical analysis basis for measurement and optimization of the interfacial mechanical properties of carbon nanotube composites.

ACKNOWLEDGEMENTS

ZC thanks CSIRO for granting permission to publish this work.

REFERENCES

[1] E. T. Thostenson, Z. F. Ren and T. W. Chou, Advances in the science and technology of carbon nanotubes and their composites: a review, *Composites Science and Technology*, **61**(13), 2001, pp. 1899-1912.

[2] J. A. Rogers, T. Someya and Y. G. Huang, Materials and mechanics for stretchable electronics, *Science*, **327**(5973), 2010, pp.1603-1607.

[3] K. S. Novoselov, V. I. Fal'ko, L. Colombo, P. R. Gellert, M. G. Schwab and K. Kim, A roadmap for graphene, *Nature*, **490**(7419), 2012, pp. 192-200.

[4] R. J. Young, I. A. Kinloch, L. Gong and K. S. Novoselov, The mechanics of graphene nanocomposites: A review, *Composites Science and Technology*, **72**(12), 2012, pp. 1459-1476.

[5] L. S. Schadler, S. C. Giannaris and P. M. Ajayan, Load transfer in carbon nanotube epoxy composites, *Applied Physics Letters*, **73**(26), 1998, pp. 3842-3844.

[6] D. Qian, E. C. Dickey, R. Andrews and T. Rantell, Load transfer and deformation mechanisms in carbon nanotube-polystyrene composites, *Applied Physics Letters*, **76**(20), 2000, pp. 2868-2870.

[7] L. Gong, I. A. Kinloch, R. J. Young, I. Riaz, R. Jalil and K. S. Novoselov, Interfacial stress transfer in a graphene monolayer nanocomposite, *Advanced Materials*, **22**(24), 2010, pp. 2694-2697.

[8] T. Jiang, R. Huang and Y. Zhu, Interfacial sliding and buckling of monolayer graphene on a stretchable substrate, *Advanced Functional Materials*, **24**(3), 2014, pp. 396-402.

[9] X.L. Gao and K. Li, A shear-lag model for carbon nanotube-reinforced polymer composites, *International Journal of Solids and Structures*, **42**(5-6), 2005, pp. 1649-1667.

[10] L. De Lorenzis and G. Zavarise, Cohesive zone modeling of interfacial stresses in plated beams, *International Journal of Solids and Structures*, **46**(24), 2009, pp. 4181-4191.

[11] M. Kulkarni, D. Carnahan, K. Kulkarni, D. Qian and J. L. Abot, Elastic response of a carbon nanotube fiber reinforced polymeric composite: A numerical and experimental study, *Composites Part B-Engineering*, **41**(5), 2010, pp. 414-421.

[12] Y. L. Chen, B. Liu, X. Q. He, Y. Huang, and K. C. Hwang, Failure analysis and the optimal toughness design of carbon nanotube-reinforced composites, *Composites Science and Technology*, **70**(9), 2010, pp. 1360-1367.

[13] Y. Y. Jia, Z. R. Chen and W. Yan, A numerical study on carbon nanotube-hybridized carbon fibre pullout, *Composites Science and Technology*, **91**, 2014, pp. 38-44.

[14] S. K. Ryu, T. F. Jiang, J. Im, P. S. Ho and R. Huang, Thermomechanical failure analysis of through-silicon via interface using a shear-lag model with cohesive zone, *IEEE Transactions on Device and Materials Reliability*, **14**(1), 2014, pp. 318-326.

[15] Y. Y. Jia, Z. R. Chen and W. Yan, A numerical study on carbon nanotube pullout to understand its bridging effect in carbon nanotube reinforced composites, *Composites Part B-Engineering*, **81**, 2015, pp. 64-71.

[16] Z.R. Chen and W. Yan, A shear-lag model with a cohesive fibre-matrix interface for analysis of fibre pull-out, *Mechanics of Materials*, **91**, 2015, pp. 119-135.
[17] G. D. Guo and Y. Zhu, Cohesive-shear-lag modeling of interfacial stress transfer between a monolayer graphene and a polymer substrate, *Journal of Applied Mechanics-Transactions of the ASME*, **82**(3), 2015, 031005.
[18] Z. H. Dai, G. R. Wang, L. Q. Liu, Y. Hou, Y. G. Wei and Z. Zhang, Mechanical behavior and properties of hydrogen bonded graphene/polymer nano-interfaces, *Composites Science and Technology*, **136**, 2016, pp. 1-9.
[19] L. N. McCartney, New theoretical-model of stress transfer between fiber and matrix in a uniaxially fiber-reinforced composite, *Proceedings of the Royal Society of London Series A-Mathematical Physical and Engineering Sciences*, **425**(1868), 1989, pp. 215-244.
[20] J.A. Nairn, Generalized shear-lag analysis including imperfect interfaces, *Advanced Composites Letters*, **13**(6), 2004, pp. 263-274.